ELSEVIER

Journal of Power Sources 104 (2002) 13–23

JOURNAL OF POWER SOURCES

www.elsevier.com/locate/jpowsour

Analysis of the interface between lithium and organic electrolyte solution

Ken-ichi Morigaki*

Battery Research and Development Center, Matsushita Electric Industrial Co. Ltd., 1 Matsushita-cho, C/o Room, Moriguchi, Osaka 570-8511, Japan

Received 2 August 2000; received in revised form 26 April 2001; accepted 9 July 2001

Abstract

The interfacial reaction between lithium and 1 mol/dm^3 $LiPF_6$/EC + DMC solution was investigated by in situ Fourier transform infrared (FTIR) spectroscopy. The double modulation FTIR (DMFTIR) spectra after immersion for 1 and 15 h indicate the formation of new reduction products of the solvent on lithium. Morphological changes by the surface reaction were observed after immersion for 15 h by in situ AFM. Some parts of lithium surface were raised as particles or ridgelines. Measurements of force–distance curves in AFM observation were carried out to investigate the interfacial layer on lithium. An attempt was also made to estimate the thickness of passive layer on lithium, and whether polymeric layer exists on lithium or not. The interfacial layer on lithium in $LiPF_6$/EC + DMC solution was estimated to be about 5 nm in thickness. The morphology of deposited lithium in $LiPF_6$/EC + DMC was investigated and compared with that in $LiClO_4$/EC + DMC by in situ AFM. The morphological change of lithium deposition in the initial stages occurred mainly on the ridgelines.
© 2002 Elsevier Science B.V. All rights reserved.

Keywords: Lithium battery; Lithium; Interfacial layer; In situ analysis; AFM; FTIR

1. Introduction

The development of small rechargeable batteries is proceeding rapidly. Portable appliances, such as cellular phones, camcorders and notebook personal computers, have become more popular and the demand for small rechargeable batteries as power sources is increasing. Lithium-ion batteries have impressively developed, because their performances meet the demands of appliances. Moreover, batteries for portable appliances are required to be smaller and thinner in size and higher in capacity corresponding to recent developments of electronics. Lithium-ion batteries use the intercalation of lithium into graphite matrix as the negative electrode reaction. Accordingly, the capacity of lithium-ion batteries is limited by the restraint of the theoretical capacity of lithium–graphite intercalation compound, which is 372 mAh/g for C_6Li.

Therefore, it is highly expected that rechargeable lithium batteries using lithium metal negative electrode will offer higher specific energy density, since lithium has a high theoretical capacity over 3000 mAh/g. One of the difficulties in practical use of rechargeable lithium batteries is the poor rechargeability of lithium electrode, which is mainly due to the formation of lithium dendrites during charging process. Because the surface of electrode is covered by surface passive layer, the layer influences the electrochemical behavior and phenomenon on lithium. Therefore, it is very important to understand the surface reaction and the surface passive layer and to control lithium surface for the development of rechargeable lithium batteries. Many studies on rechargeable lithium batteries have been reported up to the present, and the following three models for the surface passive layer on lithium have been suggested.

1. Solid electrolyte interface (SEI) model [1].
2. Polymer electrolyte interface (PEI) model [2].
3. Two-phase model (combining above two models) [3].

Although many researchers are studying on the surface passive layer and the phenomenon of lithium surface, it does not seem that the surface layer on lithium and the mechanism of lithium dendrite formation have been clarified sufficiently, and more investigations of the surface structure of lithium are required. The problems in studies on lithium and lithium deposition are that they are very sensitive to H_2O, CO_2, and O_2 in organic electrolyte solutions and in the air, and that the surface of lithium is not homogeneous and uniform. Therefore, in situ analysis and microscopic analysis are necessary for the study on lithium chemistry. Surface chemistry of lithium in organic electrolyte solution has been investigated indirectly using in situ and ex situ Fourier transform infrared (FTIR) spectroscopy by Aurbach and co-workers [4–8]. It was reported that organic carbonate solvents are reduced to lithium alkylcarbonates.

* Fax: +81-6-6998-3179.
E-mail address: morigaki@ctmo.mei.co.jp (K.-i. Morigaki).

0378-7753/02/$ – see front matter © 2002 Elsevier Science B.V. All rights reserved.
PII: S0378-7753(01)00871-0

For example, ethylene carbonate (EC) is reduced to $(CH_2COOLi)_2$, and ether-compounds are reduced to lithium alkoxides. The other surface chemistry of lithium was investigated by ex situ X-ray photoelectron spectroscopy (XPS) [9–11]. It was reported that the surface layer was covered by Li_2CO_3, Li_2O, LiOH, some organic compounds, and decomposition products of electrolyte salts, such as LiF in the case of $LiPF_6$.

Recently, scanning probe microscopy (SPM), especially, atomic force microscopy (AFM) attracts attention as a useful and effective tool for in situ analysis of the surface morphology. The author has showed that AFM observation is a useful method for in situ analysis of lithium surface and the study on lithium deposition [12–14]. The author has also studied on the interfacial reaction on copper electrode using in situ AFM and FTIR spectroscopy [15,16]. Lithium deposition on copper electrode was also investigated by in situ AFM observation by Aurbach and Cohen [17]. The morphological studies about graphite electrodes during cathodic polarization (charging process in the lithium-ion battery system) have investigated by electrochemical AFM [18–20]. Inaba and co-workers have studied the topographical changes of graphite (high oriented pyrolytic graphite (HOPG)) in organic electrolyte solutions under polarization by electrochemical STM [21–23].

In this study, surface chemistry of lithium in EC + dimetyl carbonate (DMC) solution containing 1 mol/dm^3 $LiPF_6$ is investigated by in situ double modulation FTIR (DMFTIR) spectroscopy. The morphological change of lithium surface is observed by in situ AFM. As a new trial, force–distance curve measurements are applied to assess the thickness of the interfacial layer between lithium and organic electrolyte solution. The lithium deposition is also examined by in situ AFM.

2. Experimental

EC and DMC of battery grade purchased from Mitsubishi Chemical, $LiPF_6$ of battery grade purchased from Stella Chemifa, and $LiClO_4$ of battery grade purchased from Tomiyama were used as received. The electrolyte solutions used were EC + DMC (1:1 by volume) containing 1 mol/dm^3 $LiPF_6$ or $LiClO_4$, and their water levels were kept below 50 ppm. Lithium foil (purity = 99.9%, thickness = 180 μm) purchased from Kyokuto Metal served as a working electrode. Lithium foil was also used for the counter and reference electrodes.

The optical system for DMFTIR measurements is the same as infrared reflection absorption spectroscopy (IRAS), and is shown in Fig. 1. The test cell was mounted on a NaCl optical window which had an angle of incidence of 70°. DMFTIR spectroscopy [24–26] was performed using p- and s-polarized IR beams modulated by a photoelastic modulator (PEM-90, Hinds) to enhance the sensitivity to surface species. The DMFTIR spectra data were sampled with a realtime sampling electronics (Mattson). A detector signal consists of an ac component corresponding to $(I_p - I_s)$ and a dc component corresponding to $(I_p + I_s)$, where I_p and I_s are detected intensities of the p- and s-polarized beams. As described in previous studies [14–16,24–26], $(I_p - I_s)/(I_p + I_s)$ is given as a DMFTIR spectrum. The main advantage of this technique is that $(I_p - I_s)$, which contains the absorption spectra on the electrode surface, is amplified directly by a realtime sampling electronics before digitization, resulting in a high signal-to-noise ratio. The center frequency of DMFTIR was set at 1200 cm^{-1} and the resolution of spectra was 4 cm^{-1}. About 100 FTIR measurements scans were accumulated.

AFM observation was performed with a TMX-1000 system (Topometrix). All AFM images were collected in the "contact mode" in which the probe contacted lithium surface with a constant force. An I-shaped cantilever (No. AFM1600, Topometrix) with a trigonal Si probe coated with Ni thin layer was used to measure force–distance curves in the organic electrolyte solution ($LiPF_6$/EC + DMC). The force–distance curves were measured to estimate the thickness of interfacial layers on lithium, because the polymeric layer has some interactions with the probe and influences on

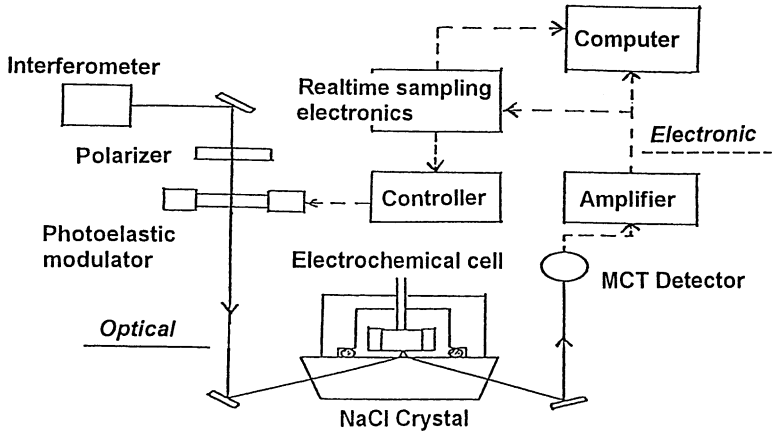

Fig. 1. Schematic configuration of DMFTIR spectroscopy.

the force–distance curve. The repulsive force (F) in force–distance curves is calculated by the following equation:

$$F = -KZ = -K\frac{d}{S}$$

where F is the repulsive force (nN), K the spring constant of a cantilever (nN/nm), Z the displaced distance by the bending, d the detection of the laser beam (nA) and S is the constant between the output of detector and the displacement of cantilever (nA/nm).

Constant S is obtained at the time of ''Tip-approach'' in AFM measurement. The ''distance'' is also set automatically at the time of ''Tip-approach''. The approach speed of the probe to the surface in force–distance curve measurements was set 1000 nm/s. Although studies on force–distance curves have not been reported so much [27–29], and especially, the interfacial layer in organic electrolyte solution is difficult and complicated to analyze, AFM measurements will make it possible to apprehend new and distinct information about the interfacial layer.

Lithium sample was set in a test-cell and immersed in organic electrolyte solution ($LiPF_6$/EC + DMC) for 25 h. Each FTIR or AFM measurement was conducted in situ without any other treatments. All experiments were performed in a dry-air atmosphere at room temperature.

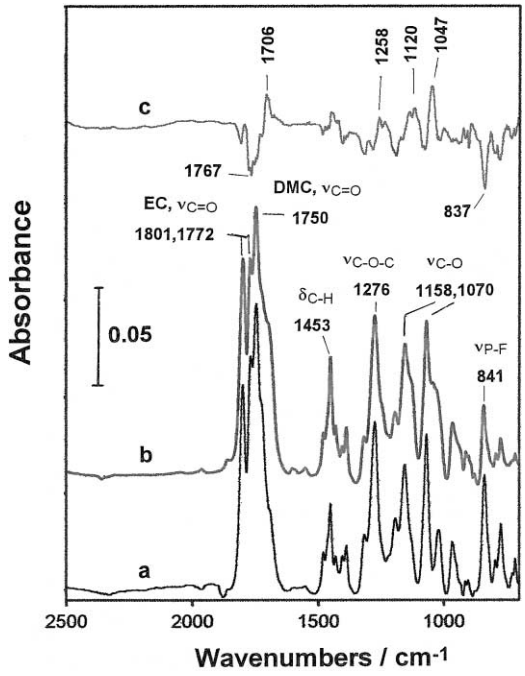

Fig. 2. Comparison between DMFTIR spectra of LiPF6/EC + DMC: (a) on copper; and (b) on lithium at OCV state; with (c) subtractive spectrum between them.

3. Results and discussion

A comparison between DMFTIR spectra of $LiPF_6$/EC + DMC on copper and on lithium at open circuit voltage (OCV) is shown in Fig. 2, together with a subtractive spectrum (Fig. 2c) between them. The open circuit voltage of copper electrode was about 3.0 V versus Li/Li^+ and that of lithium was 0 V. Although both DMFTIR spectra look very similar, upward peaks are observed at 1706 and 1047 cm^{-1}, and downward peaks at around 1760 and 837 cm^{-1} in the subtractive spectrum. The downward broad peak at around 1760 cm^{-1} seems to consist of a few peaks of the C=O asymmetric stretching vibrations ($\nu_{C=O}$) of the solvents (EC; 1773 cm^{-1} and DMC; 1751 cm^{-1}), and the peak at 837 cm^{-1} is assigned to δ_{OCO2} of EC and DMC [8]. The upward peaks at 1706 and 1047 cm^{-1} are also assigned to $\nu_{C=O}$ and ν_{C-O}, respectively, of lithium alkylcarbonate ($ROCO_2Li$) [8]. Therefore, EC and DMC were reduced on lithium surface to form lithium alkylcarbonate.

The changes of IRAS spectra on lithium in $LiPF_6$/EC + DMC solution with immersion time are shown in Fig. 3. It was reported that the surface of lithium was changed morphologically after 24 h immersion in $LiClO_4$/PC solution [13,14]. Therefore, the reaction of the electrolyte solution will occur within 24 h on lithium. IRAS spectrum 3a (Fig. 3a) (after 1 h) was obtained using the interferogram measured just after immersed in the electrolyte solution as a reference, and spectra 3b–e (Fig. 3b–e) were obtained using the former interferograms as references. The characteristic peaks of CO_2 in the solution were observed at 2360 and 2340 cm^{-1} [15]. Although the test cell for in situ FTIR spectroscopy had insufficient air tightness, the increase of the CO_2 peak indicates that the decomposition of solvents occurred. In spectrum 3a (Fig. 3a) (immersion after 1 h), the peaks of CO_2 increased and many other peaks of solvents decreased, which indicates that the decomposition of solvents occurred on lithium. In spectrum 3d (Fig. 3d) (after 15 h), the peaks of CO_2 changed downward. Other downward peaks are observed at 1247, 1446, and 909 cm^{-1}, and upward peaks appeared at 1760, 1673, 998 and 801 cm^{-1}. The upward peaks at around 1673 and 1760 cm^{-1} are ascribed to $\nu_{C=O}$ of $ROCO_2Li$, and the peak at 998 cm^{-1} to ν_{C-C} of $ROCO_2Li$ [8,15]. The peak at 1247 cm^{-1} is often observed in IRAS spectra in solutions containing EC and assigned to ν_{C-O-C} of EC. Therefore, EC was reduced to $ROCO_2Li$, and CO_2 decreased and might react on lithium surface, which results in a morphological change as shown later. Spectrum 3f (Fig. 3f) shows a decrease of CO_2 peaks with upward peaks at 1668 and 995 cm^{-1}. This result indicates that the interfacial reactions continuously occurred on lithium, which formed $ROCO_2Li$ in the solution.

The changes of DMFTIR spectra on lithium in $LiPF_6$/EC + DMC solution with immersion time were also measured, but the dominant peaks from 1800 to 1650 cm^{-1} were superimposed with several peaks. These peaks are assigned to C=O asymmetric stretching vibrations of solvents (EC and DMC) and reduction products, such as $ROCO_2Li$. Some changes in these peaks were observed with immersion

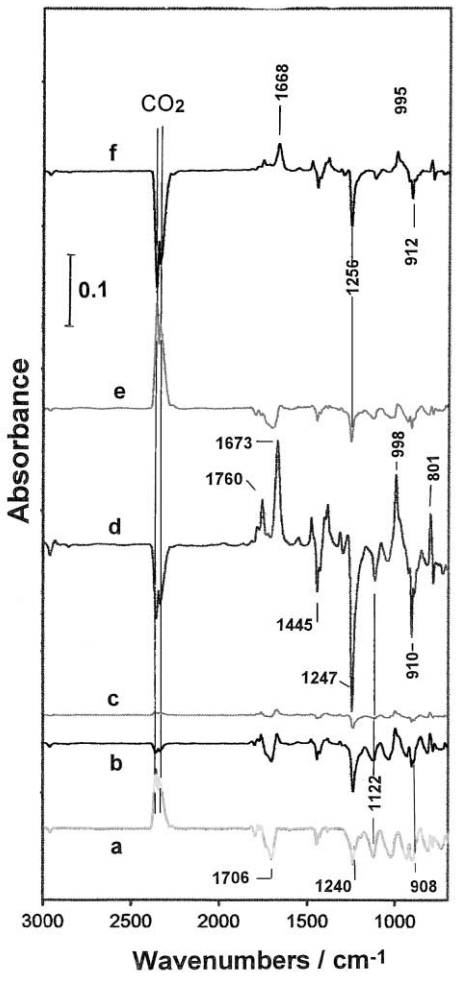

Fig. 3. IRAS spectra of LiPF6/EC + DMC on lithium with immersion time after (a) 1 h; (b) 3 h; (c) 5 h; (d) 15 h; (e) 20 h; and (f) 25 h.

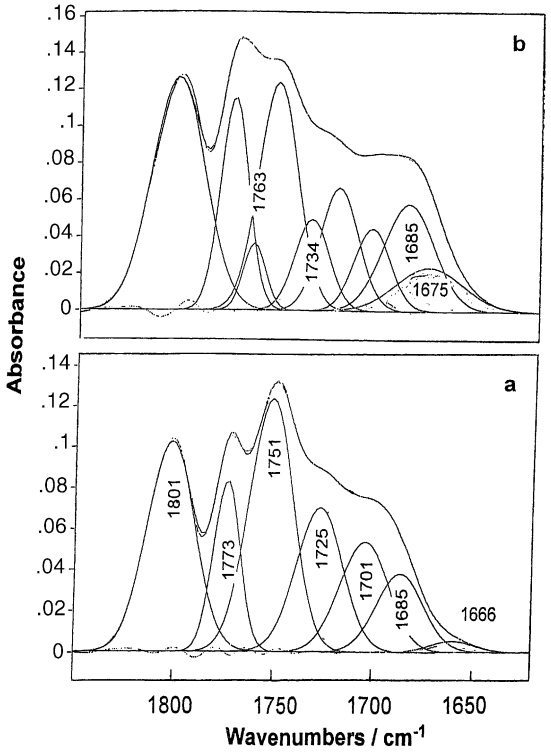

Fig. 4. Results of wave analysis for the peaks of C=O asymmetric stretching vibration in DMFTIR spectrum after 15 h.

time, but they were very complicated. Wave analysis for the peaks from 1850 to 1600 cm^{-1} was performed using a curve-fitting program GRAMS/386 (Galactic) [16]. The results of wave analysis are shown in Table 1. Typical curve fitting results for the spectra obtained at the initial state and after 15 h immersion are shown in Fig. 4. A new peak appeared at 1732 cm^{-1} in the spectrum after 1 h immersion and another new peak appeared at 1763 cm^{-1} in the spectrum after 15 h. On the other hand, the ratio of a peak corresponding to DMC (1751 cm^{-1}) and those of peaks at around 1724 and 1705 cm^{-1} decreased with immersion time. Although the new peaks were observed after immersion and they are ascribed to $\nu_{C=O}$ of $ROCO_2Li$, the ratio of new peaks was relatively small (about 10%). The peaks at 1685 cm^{-1} and around 1670 cm^{-1} increased with immersion time, and they are also ascribed to $\nu_{C=O}$ of $ROCO_2Li$ [15].

Table 1
Results of wave analysis for the peaks of C=O asymmetric stretching vibration in DMFTIR spectra, as each center peak and its ratio

Time (h)		I (EC)	II (EC)	III	IV (DMC)	V	VI	VII	VIII	IX
0	Center (cm^{-1})	1801	1773	–	1751	–	1725	1701	1685	1666
	Share (%)	23.5	10.5	–	27.3	–	16.9	13.4	6.3	2.1
1	Center (cm^{-1})	1801	1773	–	1751	1732	1723	1705	1686	1667
	Share (%)	24.4	10.3	–	28	5.3	7.9	14.1	7.5	2.3
3	Center (cm^{-1})	1801	1773	–	1751	1731	1720	1703	1685	1668
	Share (%)	25.5	10.2	–	28.9	5.3	8.8	11.3	7.5	2.4
5	Center (cm^{-1})	1801	1773	–	1751	1732	1722	1705	1687	1667
	Share (%)	25.5	10	–	28.9	3.3	10	10.2	9.9	2.2
15	Center (cm^{-1})	1801	1773	1763	1751	1737	1725	1705	1685	1666
	Share (%)	25.2	12.6	3.1	18.6	3.1	12.6	8.9	13.2	2.7
20	Center (cm^{-1})	1801	1773	1762	1751	1734	1720	1703	1685	1675
	Share (%)	25.5	12.5	3.7	17	8	10	6.9	9.3	7.1
25	Center (cm^{-1})	1801	1773	1763	1751	1734	1720	1703	1685	1675
	Share (%)	25.3	12.6	3.1	18.9	6.6	9.9	6.2	11.3	6

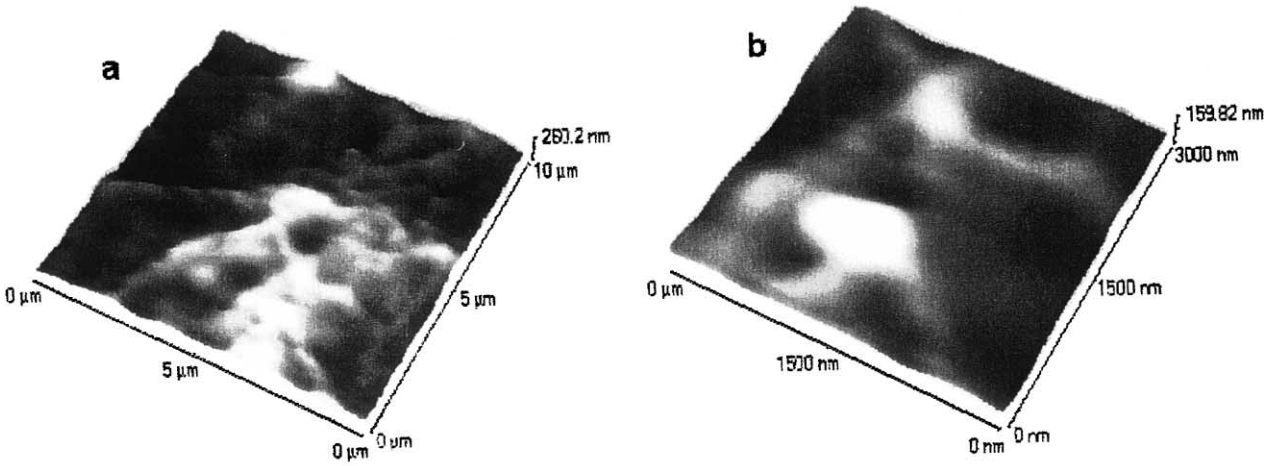

Fig. 5. AFM images of lithium surface in $LiPF_6$/EC + DMC: (a) 10 μm × 10 μm; (b) 3000 nm × 3000 nm.

However, they were observed at the initial state and their ratios were small. On the other hand, the 1801 cm^{-1} peak, which is assigned to $\nu_{C=O}$ of EC [8,15], remained constant and became the dominant peak during immersion. Therefore, the surface of lithium was covered with the reduction products ($ROCO_2Li$), but the ratios of the products were smaller than those of solvents.

Fig. 5 presents typical AFM images (10 μm × 10 μm and 3000 nm × 3000 nm areas) of lithium surface just after immersed in $LiPF_6$/EC + DMC. AFM images were treated by a leveling process and a modification of irregular traces during scanning. Lithium surface consisted of ridgelines about 300 nm in width, raised particles and the other parts. The raised particles were about 0.6 μm in length and 100 nm in height. It is observed that raised part exists for the most part of lithium surface in $LiPF_6$/EC + DMC.

Morphological changes of lithium surface (20 μm × 20 μm area) with immersion time are presented in Fig. 6. Fig. 6c shows that the morphology of lithium surface changed after 15 h in $LiPF_6$/EC + DMC. The morphological changes on lithium surface in $LiPF_6$-solution were more apparent than those of in $LiClO_4$-solution [13]. Lithium surface looked like an assemblage of particles of 1–2 μm in size. After 25 h, it was observed that particles combined and made complicated

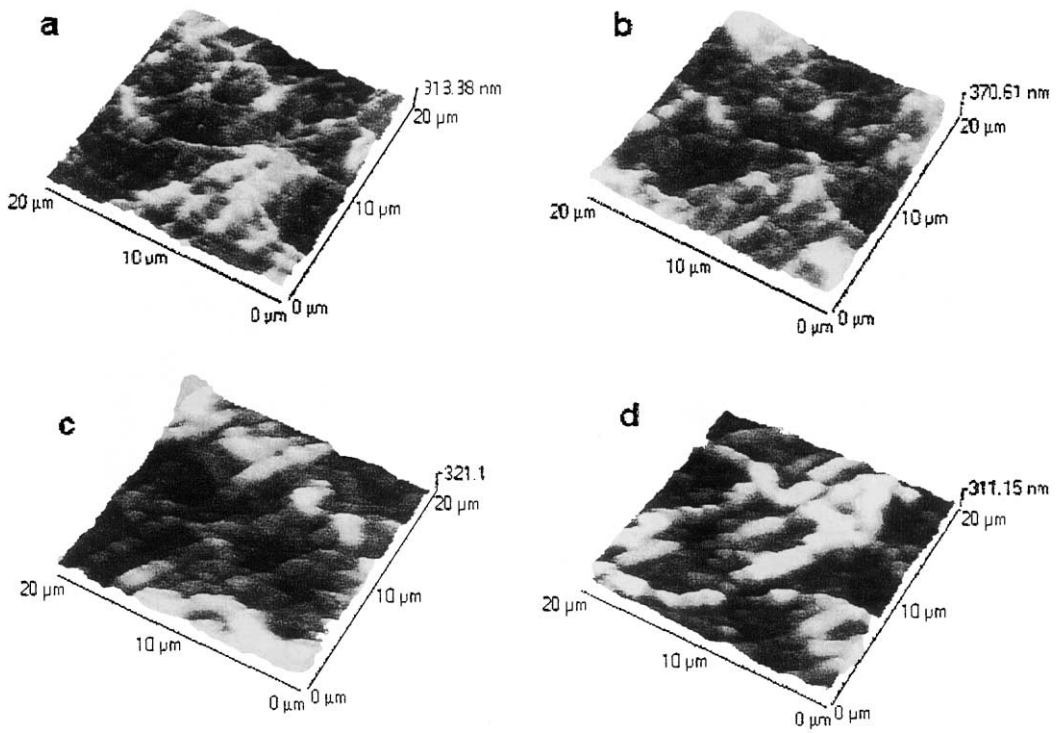

Fig. 6. Morphological changes of lithium with immersion time in $LiPF_6$/EC + DMC. AFM images (20 μm × 20 μm): (a) at the initial state; (b) after 5 h; (c) after 15 h; (d) after 25 h.

ridgelines. Therefore, EC and DMC were reduced on lithium surface to produce lithium alkylcarbonates ($ROCO_2Li$), which have the peak of $\nu_{C=O}$ at 1706 cm^{-1} and the peak of ν_{C-O} at 1047 cm^{-1} [8], as shown in Fig. 2.

In order to estimate the thickness of interfacial layers on lithium, the analysis of force–distance curves were examined. The force–distance curves on lithium in $LiPF_6$/EC + DMC are shown in Fig. 7. Each force–distance curve

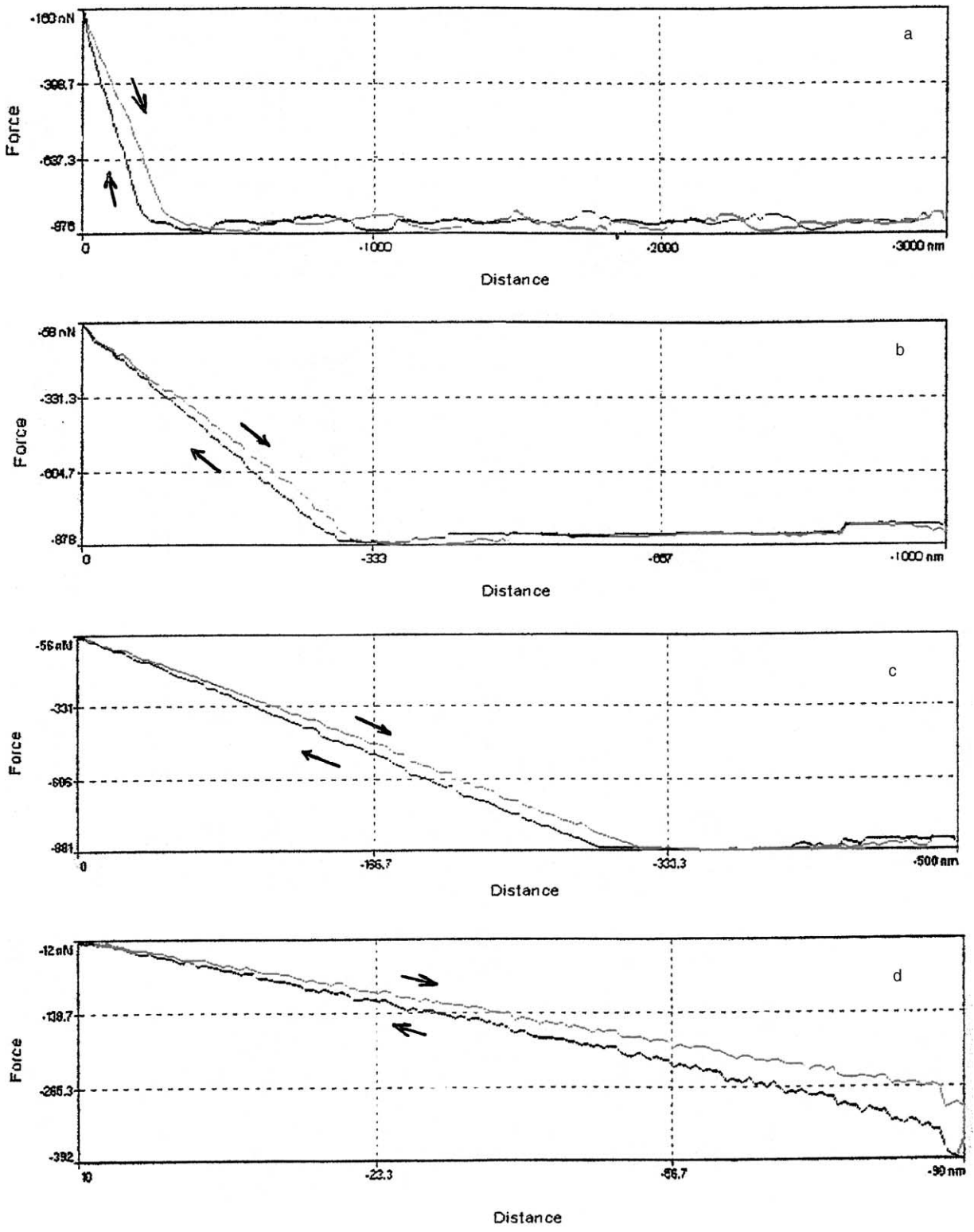

Fig. 7. Force–distance curves in the interface between lithium and electrolyte solution ($LiPF_6$/EC + DMC) at the initial state. Approaching speed: 1000 nm/s, distance: (a) 0–3000 nm; (b) 0–1000 nm; (c) 0–500 nm; (d) −10 to 90 nm.

shows two traces, an approaching trace (the lower line) and a leaving trace (the upper line). Each measurement point was selected on the raised parts in the AFM image, because the probe must precisely contact the surface. If the surface passive layer consisting of polymeric compounds exists, they will interact somewhat with the probe as adhesive, and make some difference in the force–distance curve. An oscillation, which is caused by the interference between reflections from the cantilever and the surface, was observed in the region where the probe and sample were not in contact, such as the right-hand side in Fig. 7a and b. Each force–distance curve (except Fig. 7d) indicates that a repulsive boundary started at 320 nm from the surface, assuming that the point of 0 distance is the surface of sample on this study, and no attractive region existed. It is unexpected that the slope of force–distance curve at leaving was more gradual than that at approaching, that is, the trace lies on the right-hand side of the approaching trace. It was confirmed that this phenomenon was not caused by the piezo hysteresis or the swelling or deformation of lithium. Therefore, the repulsive force due to electrostatic friction acts in the interface where ionic density is very high. The force–distance curves in Fig. 7b and c show that the change of slope and the separation of approaching and leaving traces occur at 42–43 nm from the surface. Nevertheless, the force–distance curve of Fig. 7d indicates no distinct and significant changes at around 40 nm.

Fig. 8 presents the change in force–distance curves with time in the case where the distance is 1000 nm from the surface. The measured points were not the same, because lithium surface changed morphologically by the surface reaction and the drift of scanner and other factors, such as vibration. Accordingly, similar points were selected for measurements, such as the raised part, as possible. Triangle symbols (▼) in Fig. 8 indicate the points at the distance of 100 and 200 nm from the surface. After immersion for 15 h, the force–distance curve showed a change of the repulsive boundary (Fig. 8c). The repulsive area (interface on lithium) started from 320 nm at the initial state, however, it moved from 210 nm after 15 h, and about 295 nm after 25 h. This phenomenon is related with the results of spectroscopy (Fig. 3) and morphology (Fig. 6), and both results showed that distinct changes occurred after 15 h. Each force–distance curve shows that the slope at leaving is more gradual than that at approaching. Accordingly the interface (layer) acted more repulsively at leaving process than that at approaching.

The changes in force–distance curves in close proximity to the surface are shown in Fig. 9. In these measurements, the probe (cantilever) approached from the distance of 90 nm and after it contacted with the surface, Z-scanner moved more 10 nm. The probe did not stick into lithium surface and the cantilever may be bending, because no traces, cavities or holes were observed in AFM images after these measurements. Triangle symbols (▼) in the figure indicate the points at the distance of 5 and 30 nm from the surface. In this condition, each force–distance curve showed very similar trace, in spite of a change in the slope observed in Fig. 8. Each curve also shows that the approaching trace and the leaving trace are consistent with each other in the range from about 0 to −10 nm, and then the leaving trace lies on the right-hand side of that at approaching. Consequently, in the interfacial layer, the repulsive force is superior to the adhesive force of the surface layer if the polymeric layer exists on lithium. In order to estimate an inflection point, result of the extrapolation for the slope of leaving trace indicates the point about 5 nm distant from the surface. Therefore, the thickness of interfacial layer on lithium may be about 5 nm. The interfacial layer is not tightly constructed, however, it is like a precipitation of reduction products. Sometimes, inflection points or plateaus appeared on the force–distance curves, but they disappeared in the second or the third measurement. In the case that the probe was contaminated, both the force–distance curve and AFM image became indistinct and obscure.

Because it is expected that morphological changes during immersion affect deposition of lithium, the electrodeposition of lithium was conducted after immersion for 25 h in $LiPF_6$/EC + DMC and in $LiClO_4$/EC + DMC. The morphological change by lithium deposition in $LiPF_6$/EC + DMC is shown in Fig. 10, together with line-profiles. Lithium was deposited galvanostatically at 1.0 mA/cm^2 and charge of 0.18 C/cm^2 was passed. Triangle symbols (▼) in line-profile curves indicate the same positions (the same distances). The observed area (3000 nm × 3000 nm) was a part of the ridgeline and consisted of many raised particles. Morphological changes by deposited lithium mainly occurred on complicated ridgelines and raised particles. A typical morphological change was observed as a formation of raised particles as is seen at the upper side in AFM image (Fig. 10c). These raised particles of deposition are observed at the left-hand side and the center in the line-profile (Fig. 10d). The result of line-profile is interesting, because the changes by deposition occurred at the highest part (▼1) and at a lower part (the right-hand side of ▼2). The line-profiles also show that some parts remained unchanged after deposition. Morphological changes by deposition were not uniform, but localized, which is in agreement with the results in the previous papers [13,14], however, the deposition occurred not only at higher parts, but also at lower parts. The results of morphological changes, especially those in the line-profiles, suggest that the growth of deposited lithium occurs particularly on the ridgelines, which changed during immersion in the solution.

As a comparison, morphological changes by lithium deposition in $LiClO_4$/EC + DMC are shown in Fig. 11 together with line-profiles. The conditions for deposition were the same as those for the $LiPF_6$-system. Surface morphology of lithium in the $LiClO_4$-solution was observed like agglomerates of small particles (about 200 nm in size). Morphological changes by deposition were observed as a formation of large raised particles (500–700 nm in size) on

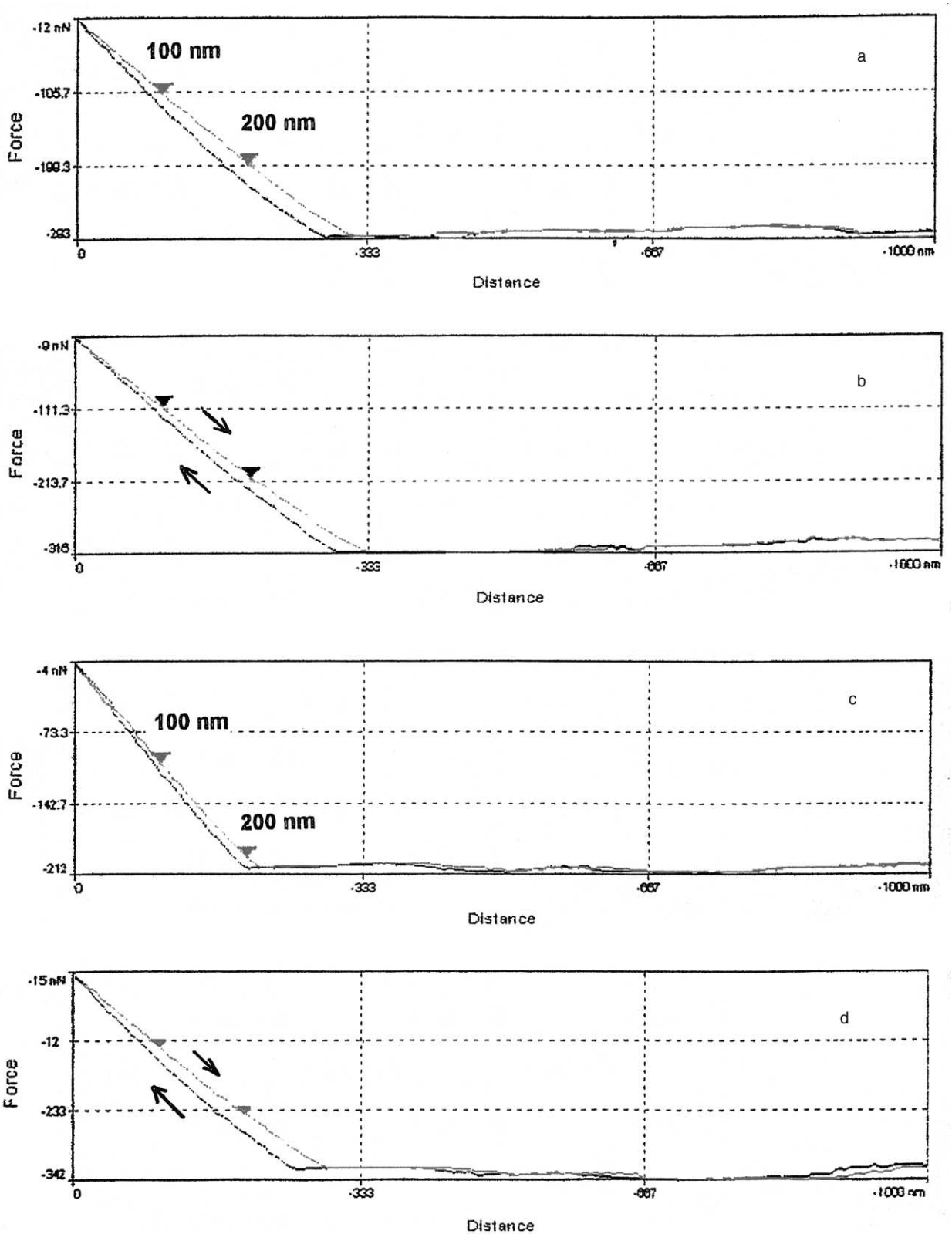

Fig. 8. Changes in force–distance curves on lithium in $LiPF_6$/EC + DMC: (a) at the initial state; (b) immersion after 3 h; (c) after 15 h; and (d) after 25 h. Conditions; approaching speed: 1000 nm/s, distance: from 1000 nm to the surface.

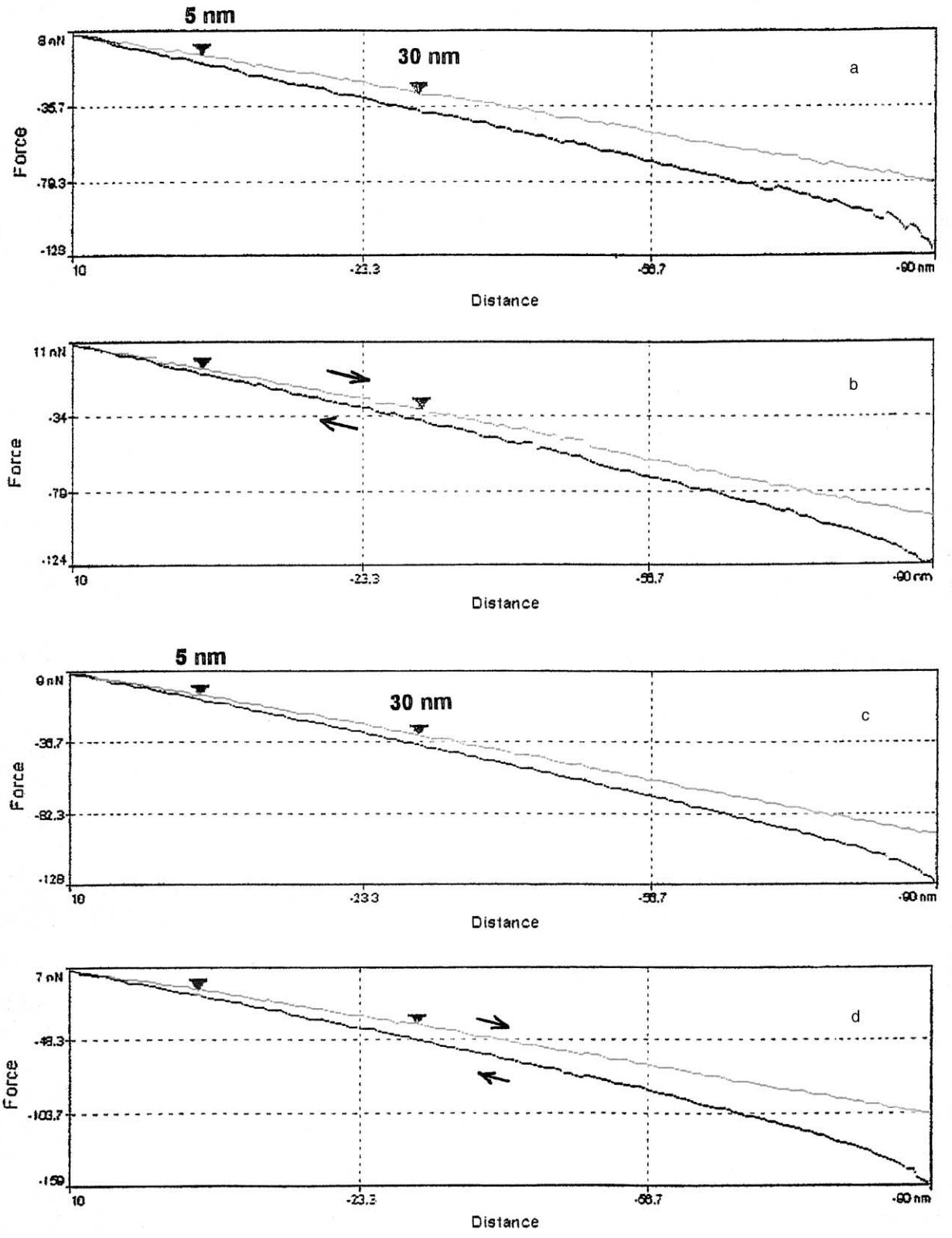

Fig. 9. Changes in force–distance curves near the surface of lithium in $LiPF_6$/EC + DMC: (a) at the initial state; (b) immersion after 3 h; (c) after 15 h; and (d) after 25 h. Conditions; approaching speed: 1000 nm/s, distance: from 90 nm to the surface (−10 nm).

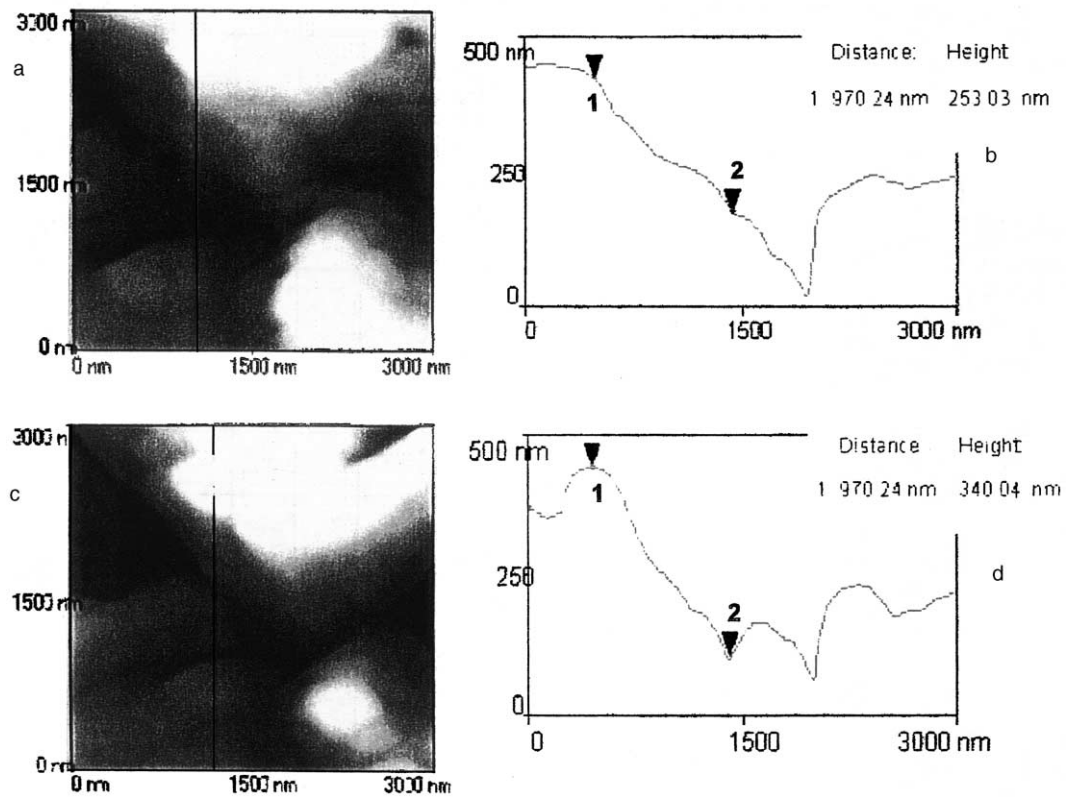

Fig. 10. AFM images and (b, d) the line analysis of lithium deposition in $LiPF_6$/EC + DMC. Condition; current density: 1 mA/cm^2, amount of deposition: 0.3 C/cm^2, (a, b) before deposition; (c, d) deposited lithium.

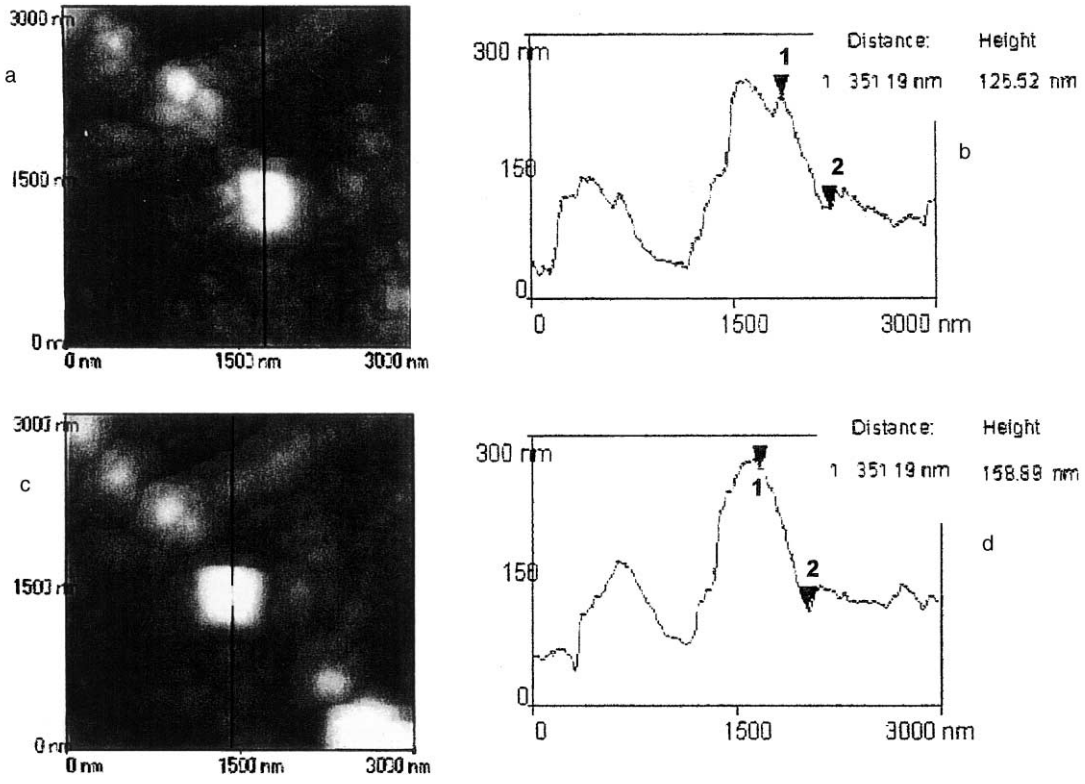

Fig. 11. AFM images and (b, d) the line analysis of lithium deposition in $LiClO_4$/EC + DMC. Condition; current density: 1 mA/cm^2, amount of deposition: 0.3 C/cm^2, (a, b) before deposition; (c, d) deposited lithium.

the ridgeline (Fig. 11c). The morphological changes were similar to those in the $LiPF_6$-solution, that is, some parts were raised and the other parts were unchanged. A distinct morphological change due to deposition occurred on the ridgelines, which were raised after immersion in the electrolyte solution. The other parts of surface, which were unchanged after immersion, remained unchanged even after the deposition. Previous studies [13,14] on lithium surface by scanning auger electron microscopy (SAM) indicated that the reaction on the ridgelines or the grain boundaries is mainly the decomposition of lithium salt (anion). It was also shown that many defects and dislocations exist in the ridgelines and grain boundaries. Lithium ions move through these defects and dislocations in the ridgelines and thereby the morphological changes by deposition occur near the ridgelines.

4. Conclusions

The DMFTIR spectroscopy on lithium shows that new peaks appeared at 1732 and 1763 cm^{-1} during immersion in $LiPF_6$/EC + DMC. They are ascribed to $\nu_{C=O}$ of the reduction products of solvents, which are lithium alkylcarbonates, and appeared after immersion for 1 and 15 h. On the other hand, the IRAS spectra indicated the dissolution of such reduction products. Wave analysis for DMFTIR spectra on lithium was performed to investigate surface reaction products and surface layer, the results indicated that the amount of reduction products was relatively small and after 25 h immersion the dominant surface species was EC.

AFM observation showed that surface morphological changes, which were caused by the surface reaction between lithium and electrolyte solution, occurred after immersion for 15 h. Lithium surface became rougher and complicated by immersion. The change in the force–distance curve also indicated that a change in the interface occurred after 15 h. However, the area where an attractive force or adhesive interaction acts, was not observed in force–distance curves from the initial state to after 25 h immersion.

Correspondingly, the surface layer on lithium consisted of a precipitation of lithium alkylcarbonates which are the reduction products of EC and DMC, and if the surface passive layer or the polymeric interfacial layer exists on lithium, it will be within the thickness of 5 nm based on the results of force–distance curves in AFM measurements.

Distinct morphological changes by deposition occurred on ridgelines, which had been raised during immersion in the electrolyte solution. The other parts of the surface, which had been unchanged during immersion, remained unchanged even after deposition. Consequently, the initial growth of deposited lithium occurs on the part of ridgelines and raised particles.

Acknowledgements

The author is indebted to the New Energy and Industrial Technology Development Organization for their support to this study.

References

[1] E. Peled, J. Electrochem. Soc. 126 (1979) 2047–2051.
[2] J. Thevenin, J. Power Sources 14 (1985) 45–51.
[3] J.G. Thevenin, R.H. Muller, J. Electrochem. Soc. 134 (1987) 273–280.
[4] D. Aurbach, M.L. Daroux, P.W. Faguy, E. Yeager, J. Electrochem. Soc. 134 (1987) 1611–1620.
[5] D. Aurbach, M.L. Daroux, P.W. Faguy, E. Yeager, J. Electrochem. Soc. 135 (1988) 1863–1871.
[6] D. Aurbach, Y. Gofer, J. Electrochem. Soc. 138 (1991) 3529–3536.
[7] D. Aurbach, O. Chusid (Youngman), J. Electrochem. Soc. 140 (1993) L155–157.
[8] D. Aurbach, B. Markovsky, A. Shechter, Y. Ein-Eli, H. Cohen, J. Electrochem. Soc. 143 (1996) 3809–3820.
[9] G. Nazri, R.H. Muller, J. Electrochem. Soc. 132 (1985) 2050–2054.
[10] K. Kanamura, H. Tamura, Z. Takehara, J. Electroanal. Chem. 333 (1992) 127–142.
[11] K. Wang, P.N. Ross Jr., F. Kong, F. McLarnon, J. Electrochem. Soc. 143 (1996) 422–428.
[12] K. Morigaki, N. Kabuto, K. Yoshino, A. Ohta, in: Proceedings of the 35th Battery Symposium, Nagoya, Japan, 1994, pp. 83–84.
[13] K. Morigaki, N. Kabuto, K. Yoshino, A. Ohta, Power Sources 15, in: A. Attewell, T. Keily (Eds.), Proceedings of the International Power Sources Symposium Committee, 1995, pp. 267–283.
[14] K. Morigaki, A. Ohta, J. Power Sources 76 (1998) 159–166.
[15] K. Morigaki, T. Fujii, A. Ohta, Denki kagaku (presently Electrochemistry) 66 (1998) 824–830.
[16] K. Morigaki, T. Fujii, A. Ohta, Denki kagaku (presently Electrochemistry) 66 (1998) 831–837.
[17] D. Aurbach, Y. Cohen, J. Electrochem. Soc. 143 (1996) 3525–3532.
[18] K.A. Hirasawa, T. Sato, H. Asahina, S. Yamaguchi, S. Mori, J. Electrochem. Soc. 144 (1997) L81–84.
[19] K.A. Hirasawa, K. Nishioka, T. Sato, S. Yamaguchi, S. Mori, J. Power Sources 69 (1997) 97–102.
[20] A.C. Chu, J.Y. Josefowicz, G.C. Farrington, J. Electrochem. Soc. 144 (1997) 4161–4169.
[21] M. Inaba, Z. Siroma, Z. Ogumi, T. Abe, Y. Mizutani, M. Asano, Langmuir 12 (1996) 1535–1540.
[22] M. Inaba, H. Yoshida, Z. Ogumi, T. Abe, Y. Mizutani, M. Asano, J. Electrochem. Soc. 142 (1995) 20–26.
[23] M. Inaba, Z. Siroma, Z. Ogumi, T. Abe, Y. Mizutani, M. Asano, Chem. Lett. (1995) 661–662.
[24] L.A. Nafie, M. Diem, Appl. Spectrosc. 33 (1979) 130–135.
[25] B.J. Barner, M.J. Green, E.I. Saez, R.M. Corn, Anal. Chem. 63 (1991) 55–60.
[26] W.N. Richmond, P.E. Faguy, R.S. Jackson, S.C. Weibel, Anal. Chem. 68 (1996) 621–628.
[27] N.A. Burnham, D.D. Dominguez, R.L. Mowery, Phys. Rev. Lett. 64 (1990) 1931–1934.
[28] D.T. Atkins, R.M. Pashley, Langmuir 9 (1993) 2232–2236.
[29] J. Mertz, O. Marti, J. Mlynek, Appl. Phys. Lett. 62 (1993) 2344–2346.